THE EFFECTS OF RIVER COUNTER-CURRENTS ON SHIPS WAKES : AN EXPERIMENTAL APPROACH.

Effets de contre-courants de rivière sur les sillages de navires : une approche expérimentale.

Clément Caplier[1], Germain Rousseaux, Damien Calluaud, Laurent David

Pprime Institute, CNRS, University of Poitiers, ISAE-ENSMA, 86962 Futuroscope Chasseneuil, France.

clement.caplier@univ-poitiers.fr, germain.rousseaux@univ-poitiers.fr, damien.calluaud@univ-poitiers.fr, laurent.david@univ-poitiers.fr

ABSTRACT

Wash waves produced by ships disintegrate river banks and coastal lines. This phenomenon of bank erosion is mainly due to the height of the waves. Various factors govern the forming of these waves and their propagation in the waterway: the geometry of the water channel, the shape and the speed of the boat, the speed and the direction of the current, etc. Although hydraulic phenomena in confined water channels are well known, the undulatory behavior of the generated waves and their interaction with the river current still remains a complex problem. Whether to study the impact of wash waves on the ship's environment or the effect of the current on their propagation in the waterway, the analysis of the ship wake is essential. This study proposes an experimental study of ship wakes generated in a towing tank, in calm water and in the presence of a counter-current. The wakes have been measured with a non-intrusive optical measurement method that gives a full and detailed reconstruction of the free surface deformation around and behind the ship. Non-usual wake patterns are identified and their analysis in both real and spectral domains allows to point out major effects of the river counter-current. An increase of waves amplitudes and length, the extension of the wash zone on river banks and the apparition of unsafe/critical/dangerous zones for navigation for other ships in the wake are identified and quantified.

KEY WORDS

Wash waves, wave field, current, bank erosion

RESUME

Les ondes de batillage déstructurent les berges des fleuves, rivières et du trait de côte. Ce phénomène d'érosion des rives est principalement lié à la hauteur des vagues générées par les navires. Plusieurs facteurs régissent la formation de ces vagues et leur propagation dans la voie d'eau : la géométrie de la voie d'eau, la forme et la vitesse du navire, la vitesse et le sens du courant, etc. Bien que les phénomènes hydrauliques dans les voies d'eau confinées sont bien connus, le comportement ondulatoire des vagues générées et leur interaction avec le courant de rivière restent un problème complexe. Que ce soit pour étudier l'impact des ondes de batillage sur l'environnement ou l'effet du courant sur la propagation des vagues dans la voie d'eau, l'analyse du sillage généré par le navire est indispensable. Cette étude propose une comparaison expérimentale des sillages de navires générés en bassin des carènes, en eau calme et en présence d'un contre-courant de rivière. Les sillages ont été mesurés avec une méthode de mesure optique non-intrusive, basée sur un principe de stéréo-vision, donnant accès à une définition complète et détaillée des champs de vagues générés. Des formes de sillages particulières sont identifiées et leur analyse à la fois dans l'espace réel et dans l'espace spectral permettent de mettre en évidence des effets important du contre-courant de rivière. Une augmentation de l'amplitude et de la longueur d'onde des vagues, l'agrandissement de la zone d'impact sur la rive et l'apparition de zones dangereuses pour la navigation des autres navires dans la voie d'eau sont identifiées et quantifiées.

MOTS-CLEFS

Ondes de batillage, champ de vague, courant, érosion des rives

[1] Corresponding author

1. INTRODUCTION

Wash waves generated by ships disintegrate river banks and shorelines. This phenomenon of bank erosion is directly linked to the height of the waves generated by the ships. Various factors govern the creation and the propagation of these waves: the configuration of the waterway (bathymetry), the shape and the speed of the boat, and the direction and the speed of the current. In the case of inland navigation, river ships are facing counter-currents or co-currents, depending on whether they navigate upstream or downstream the waterway. So the effects on the wave propagation in the waterway, particularly on the amplitudes and the wavelengths in the wave field, depend highly on this factor. Then it is essential to study the wave field behind the ship to understand the effects of the current on the wake generated by the ship in the waterway.

This study focuses on the effects of a river counter-current on the wake generated by a parabolic ship hull in a towing tank, in a shallow water configuration representative of the inland navigation. The wakes have been measured with an optical measurement method based on a stereo-refraction principle [Gomit *et al.*, 2013], giving a full and detailed reconstruction of the wave field generated around the ship. The resolution of the measured wake allows to perform a spectral analysis, following the method provided by [Gomit *et al.*, 2014 ; Caplier *et al.*, 2015], which highlights non-linear effects in the wake generated on a counter-current.

In a first step, the dispersion relation of waves in the context of wakes is presented, and the focus is made on the effect of a river current from a theoretical point of view. In a second step, the experimental setup of the study is presented through the description of the towing tank, the ship hull and the calm water and counter-current configurations. In addition, the optical measurement method based on a stereovision principle is presented. Then the wakes measured in calm water and in the presence of a counter-current will be analyzed and compared. Non-usual wake patterns are identified and their analysis in both real and spectral domains allows to point out major effects of the river counter-current. An increase of waves amplitudes and length, the extension of the wash zone on river banks and the apparition of unsafe/critical/dangerous zones for navigation for other ships in the wake are identified and quantified. In addition, non-linear effects are identified through the spectral analysis of the ship wakes.

2. THEORETICAL BACKGROUND

The wake generated by a punctual disturbance moving at the surface of a liquid has been first introduced by Lord Kelvin [1887]. This typical ship wake pattern, commonly called “Kelvin wake pattern”, describes perfectly the wake generated by ships in infinite medium (i.e. in open seas). It is composed of a diverging and a transverse wave systems, whose wave crests are respectively oblique and normal to the direction of propagation of the disturbance. The two wave systems superimpose on a cusp line on which the wave amplitudes are the highest. This line defines the envelop of the wake and forms a typical angle with the direction of propagation of the disturbance, which is called the Kelvin angle and equal to α=19.47°. When including the effect of water depth, this wave pattern is governed by the dispersion relation of waves, established by Ekman [1906, 1907] in the context of wakes, and depends on the speed of the disturbance and the water depth of the medium [Havelock, 1908 ; Inui, 1936 ; Inui, 1955 ; Crapper, 1964 ; Fang *et al.*, 2011 ; Carusotto and Rousseaux, 2013]. The dispersion relation of gravity waves on top of a fluid layer of height h, generated by a perturbation of uniform rectilinear motion, travelling at a speed U along the x-axis, is

$$\omega'(k) = \pm\sqrt{g\,k\tanh kh} - U\,k_x \ , \qquad (1)$$

where ω' is the angular frequency of the Doppler-shifted wave and $k=k'=(k_x^2+k_y^2)^{1/2}$ is the wave vector. A solution $\omega'=0$ exists for the dispersion relation, which means that the wake is stationary in the moving reference frame of the ship. Then this solution leads to

$$U^2 k_x^2 - g\sqrt{k_x^2+k_y^2}\tanh\left(h\sqrt{k_x^2+k_y^2}\right) = 0 \ , \qquad (2)$$

As regards a disturbance propagating on a current, the previous solution of the dispersion relation experiences a change of reference frame. Indeed, the relative speed of the disturbance becomes

$$\vec{v}_{relative} = \vec{U} - \vec{u} \ , \qquad (3)$$

where $\vec{U}$ is the ship speed ($|U|>0$) and $\vec{u}$ the speed of the current ($u>0$ for a co-current and $u<0$ for a counter-current). Intuitively, the solution of the dispersion relation (2) becomes :

$$\left(U+|u|\right)^2 k_x^2 - g\sqrt{k_x^2+k_y^2}\tanh\left(h\sqrt{k_x^2+k_y^2}\right) = 0 \ , \qquad (4)$$

in the case of a counter-current, and :

$$(U-|u|)^2 k_x^2 - g\sqrt{k_x^2+k_y^2}\tanh\left(h\sqrt{k_x^2+k_y^2}\right)=0 \ , \qquad (5)$$

in the case of a co-current, with $|u|$ the absolute value of the longitudinal velocity component of the current. Thus, on an undulatory point of view, the presence of a current involves a change of reference frame in the dispersion relation.

The solid lines on Figure 1 represent the solutions $\omega'=0$ of the dispersion relation in calm water, for different height-based Froude numbers $F_h=U/(gh)^{1/2}$, in the spectral domain $(O;k_x,k_y)$. For a given water depth, the increase of the ship speed leads to a pinching of the locus and a decrease of the cutoff wave number k_x^c (corresponding to $k_y=0$). The dashed lines on Figure 1 represent the solutions of the dispersion relation in the presence of a counter-current of speed $|u|=0.2\text{m.s}^{-1}$, corresponding to a height-based Froude number of perturbation $F_h'=|u|/(gh)^{1/2}=0.20$. The solutions are calculated for the same ship speeds than in calm water (each color corresponds to the same ship speed). The effects of the current on the solution of the dispersion relation consist in a shifting of the locii in the spectral space. Indeed, for a given solution in calm water, for a height-based Froude number F_h, the corresponding solution in the presence of current corresponds to the solution for a Froude number $F_h''=F_h+F_h'$. For example, the solution for $F_h=0.70$ in calm water (solid black line), becomes equal to the solution for $F_h''=0.90$ in the presence of current (the dashed black line superimposes with the solid orange line).

Although the dispersion relation describes the propagation of the gravity waves, and so the shape of the wake, it can not predict the distribution of the energy in the wake. The numerical simulations performed by Ellingsen [2014] show that the amplitudes of the waves highly depend on the incident angle of the current and its amplitude. Depending on these factors, the amplitude in the wake is distributed differently between the diverging waves and the transverse waves systems. Radial cuts in the calculated wakes show that in the presence of a counter-current, the amplitude is concentrated on the diverging waves and the wavelength of the transverse waves increases. In the presence of a co-current, the amplitude is concentrated on the transverse waves and their wavelength decreases. As regards the wash on the river banks, the experimental study of Bruschin and Dysli [1974] shows, from water level measurements on the river banks, that the energy of the wake transferred to the banks is concentrated in the presence of a co-current, and diluted otherwise.

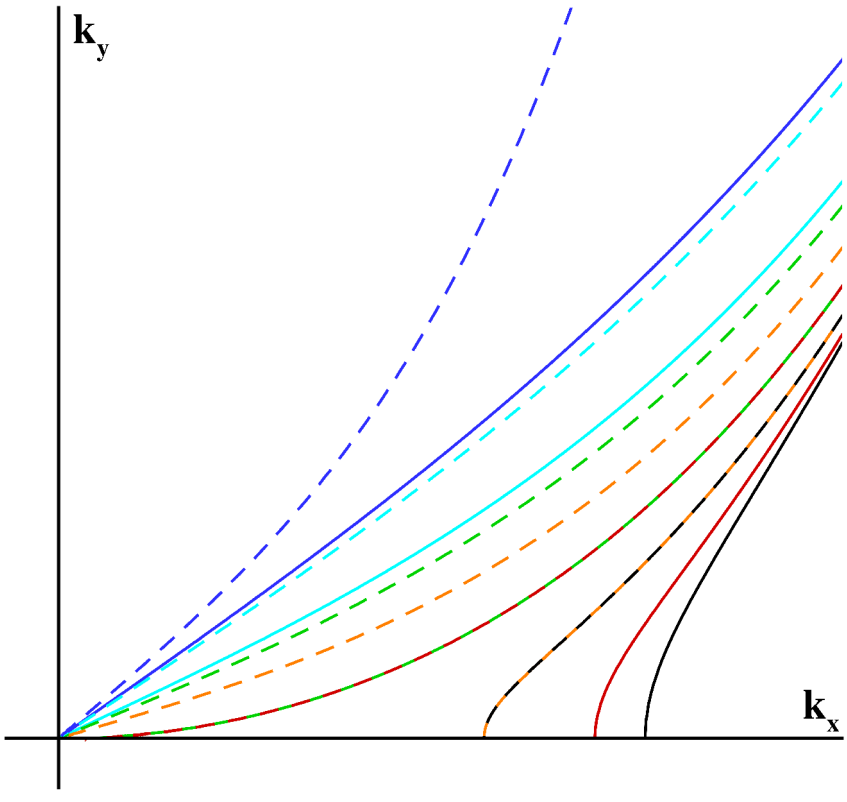

Figure 1: Solutions of the dispersion relation for different height-based Froude numbers in calm water (solid lines) and on a counter-current of speed $|u|=0.2\text{m.s}^{-1}$ (dashed lines). From right to left F_h=0.70 - 0.80 - 0.90 - 1.00 - 1.25 – 1.50.

3. EXPERIMENTAL SETUP

3.1 Towing tank and counter-current flow generation

The ship wakes have been measured in the towing tank of the Pprime Institute, of length L=20m and width W=1.5m. The hull is towed along the longitudinal axis of the canal by a towing carriage, controlled by a computer. The advancing speed U can be set up to 2.35$m.s^{-1}$ and during the trials the hull is kept fixed (so that pitch, yaw and roll are impossible). A double-bottom has been installed on the bottom of the towing tank to create a cavity in between, in which a hydraulic pump is installed. The water circulates under the double-bottom, resurfaces at the end of the canal and passes through a honeycomb to laminarize the flow (Figure 2). The water depth is set at h=0.103m for the experiments. The transversal velocity profile of the counter-current flow has been measured for z=h/2=0.051m with a SonTek ADV probe with a spatial resolution Δy=50mm at a frequency of 50Hz during 3min. per point. The measured transverse profile of the longitudinal velocity component u=f(y) shows a flat and symmetric velocity profile, with a decreasing speed close to the walls of the canal (Figure 3). Hence the waves will propagate on a lower current on the sides of the canal, so their wavelengths and amplitudes should be smaller than in the middle. For the experiments, the speed of the counter-current has been considered as $|u|$=0.20$m.s^{-1}$. The co-current case has not been studied as the set-up does not permit today to generate a flat and symmetrical velocity profile in the canal. The wakes have generated by a classical Wigley hull WH2 with a rectangular cross-section [Wigley, 1926 ; Caplier *et al.*, 2015a], of dimensions LxBxD=1.20x0.18x0.075m^3 have been measured for a ship speed U=0.45$m.s^{-1}$, corresponding to a length-based Froude number F_L=0.13 and a height-based Froude number F_h=0.45. The parameters of the experiments are summarized in the Table 1.

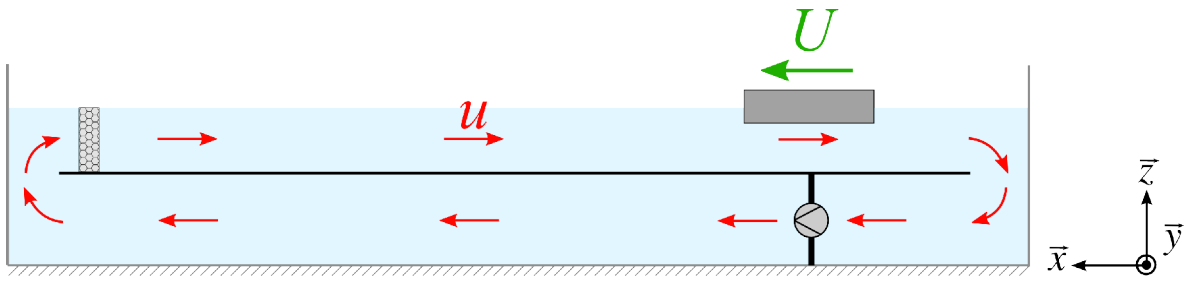

Figure 2: Schematic representation of the counter-current generation in the towing tank.

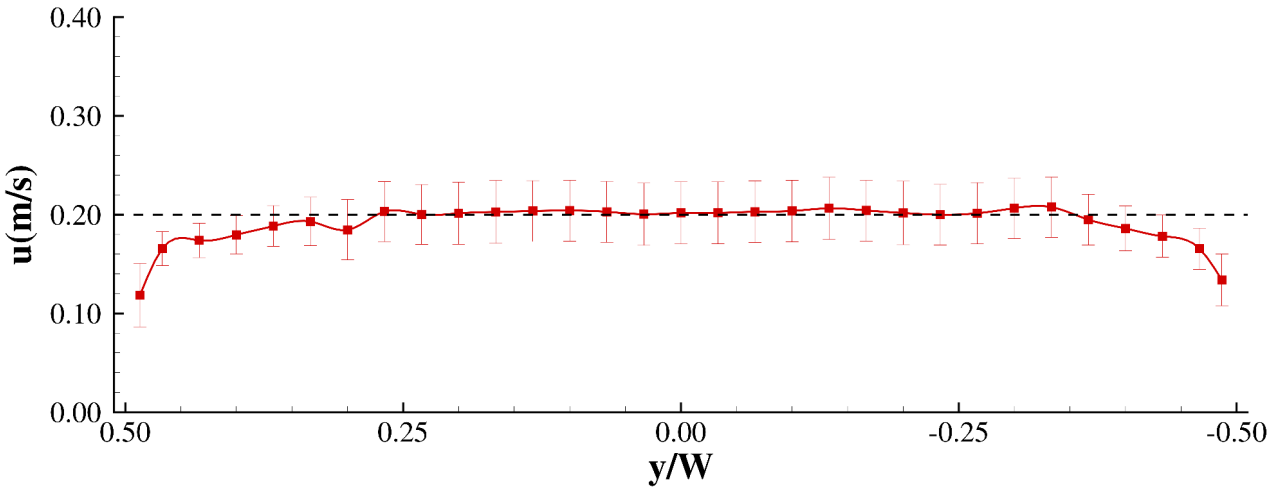

Figure 3: Transverse profile of the longitudinal velocity component u of the current. The error bars correspond to the RMS fluctuations u' around the mean velocity $\bar{u}(y)$.

	calm water	counter-current
$h(m)$	0.103	
$U(m.s^{-1})$	0.45	
F_L	0.13	
F_h	0.45	
$u(m.s^{-1})$	/	0.20

Table 1: Parameters of the experiments.

3.2 Stereo-refraction measurement method

The wakes have been measured with an optical stereo-refraction measurement method [Gomit *et al.*, 2013], based on the principle of the refraction of light due to a change of medium. The applied method consists in catching the deformations of a speckle-pattern placed under the surface of water with two cameras, and to reconstruct the free surface deformation with a dedicated algorithm. For that, two cameras Jai RM-4200CL that deliver a resolution of 2048x2048 pixels and equipped with Nikkor AF 28mm 1:2.8 lenses are placed 1.5m above the surface of water. They focus on the same zone with an opposite angle of ±15° with respect to the longitudinal axis of the canal, and ±35° with respect to the vertical axis. A speckle-pattern of dimensions 0.75x0.30m^2, covering the half-width of the waterway, is placed on the double-bottom of the canal (0.103m under the water surface at rest). The acquisition of the images is performed with a R&D Vision system, composed by the Hiris software piloted by a synchronization box EG. The cameras are synchronized with the start of the ship and the exposure time is set to 10ms and the frequency of the acquisition of the images is set at 10 frames per second (fps). The first step of the stereo-correlation method consists in the calibration of the cameras. For that, a two-dimensional target of points is displaced in the air, along the longitudinal axis of the canal and the camera models are calculated with a dedicated algorithm. Then the canal can be filled up and the images of the speckle-pattern with the water surface at rest are recorded. These images will represent the reference pattern for the reconstruction of the free surface. Then the ship is launched and the deformations of the pattern are recorded on each camera. Each run is performed three times to check the reproducibility of the measurement. Once the images have been recorded, a reconstruction algorithm based on the SLIP library [Tremblais and David, 2010] processes the image pairs. The free surface deformation is calculated at each time step with a spatial resolution of 5mm and a precision of the water level of 0.1mm. Finally, from the three wave fields calculated at each time step, a mean wave field is calculated. Then the whole wake is reconstructed around the ship hull with a dedicated reconstruction program (Figure 4).

4. RESULTS

4.1 Ship wakes in the real space

The measured ship wakes are presented on Figure 4. The top of the figure corresponds to the wake generated in calm water, where the classical Kelvin wake pattern can be identified [Kelvin, 1887]. Indeed, the wake is composed of a diverging and a transverse wave systems, reflecting on the walls of the canal. In addition, the V-shape wake envelop forms an angle close to the Kelvin angle α=19.47°. The bottom of the figure corresponds to the wake generated for the same ship speed against a counter-current. Multiple observations can be made from the comparison of the measured wakes. First, the cusp line forming the envelop of the wake widens with the counter-current, and does not form a straight line. Hence, the identification of a wake angle is compromised, contrary to the measured calm water V-shape wake. In addition, the amplitudes in the whole wake are more important, so the wave resistance increases with the counter-current. Indeed, the wave resistance is the reflect, in some extent, of the energy that has been transferred by the ship to the wake. As regards the transverse waves, their amplitude and wavelength increase drastically. A longitudinal cut in the wake for a transverse position Y/B=3.5 (close to the walls of the canal) is given on Figure 5. For the counter-current configuration, the wavelength of the transverse waves is $\lambda_1 \approx 0.3L$, whereas in calm water the wavelength is $\lambda_2 \approx 0.1L$, an increase of 30% of the wavelength for that particular speed. As regards the amplitudes of the transverse waves, the ratio between the crest-to-trough amplitude in counter-current A_1 and in calm water A_2 is A_1/A_2=5.9/1.2=4.9, corresponding to an increase of nearly 500% of the amplitude of the transverse waves. These two observations are easily understandable as the transverse waves wavelength is given theoretically by $\lambda_t=2\pi/k_t= 2\pi U^2/g$. So the higher the speed of the perturbation, the higher the transverse waves wavelength. In addition, the higher ship speed generates a perturbation of higher amplitude so more energy is transferred to the wake, increasing the waves amplitudes. The longitudinal cuts also highlight the widening of the wash zone on the banks. Indeed, in calm water, the length characterizing the distance between the first reflections of the bow and the stern wakes, $L_1 \approx 0.9L$ becomes equal to $L_2 \approx 2L$ on the counter-current, more than two times wider. This phenomenon, coupled to the increasing of the transverse wave amplitudes and the counter-current flow, would have a devastating impact on the river banks. Finally, the counter-current creates zones of high wave amplitude in the wake, especially in the middle of the waterway, for a longitudinal position $X/L \in [2.5;3.0]$. This zone could be dangerous for a example if the ship passes another one.

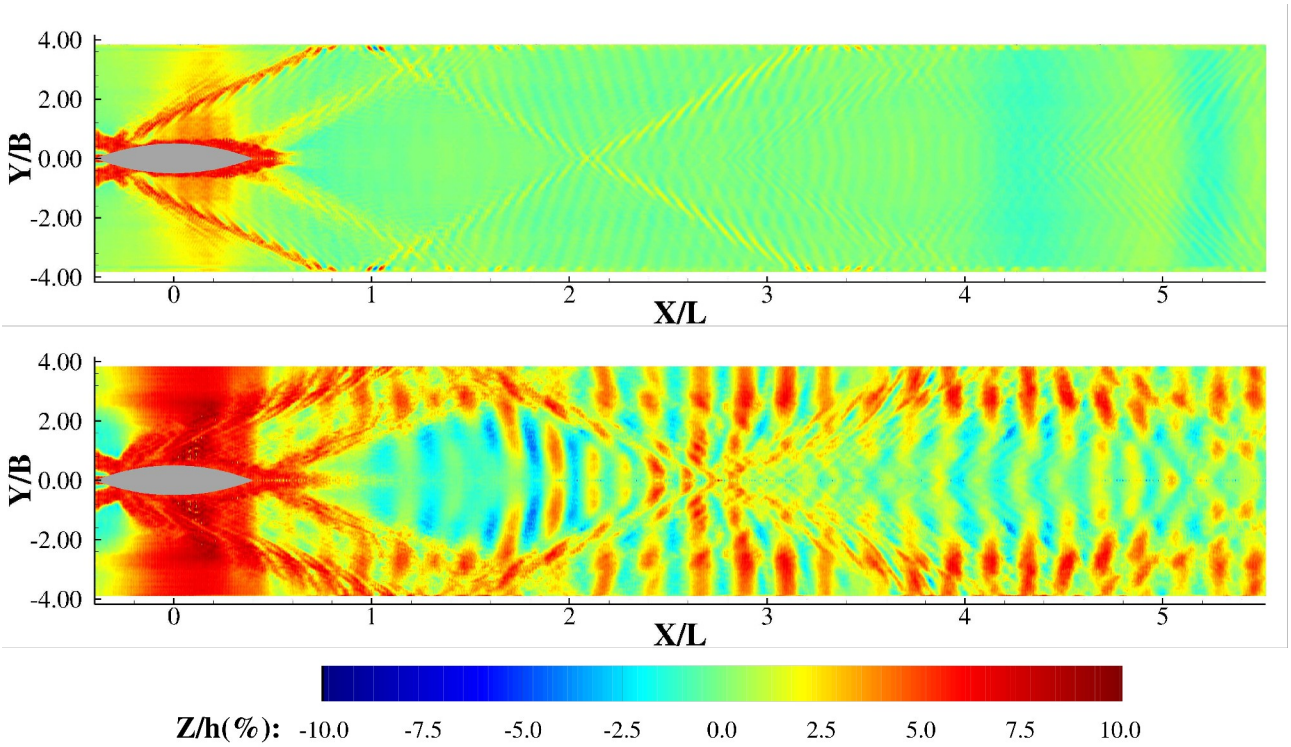

Figure 4: Ship wakes measured in calm water (top) and on a counter-current (bottom). The ship is going from right to left. The non-dimensional water depth is given as a percentage of the initial water level h. Ship speed: U=0.45$m.s^{-1}$ – Counter-current speed : $|u|$=0.20$m.s^{-1}$.

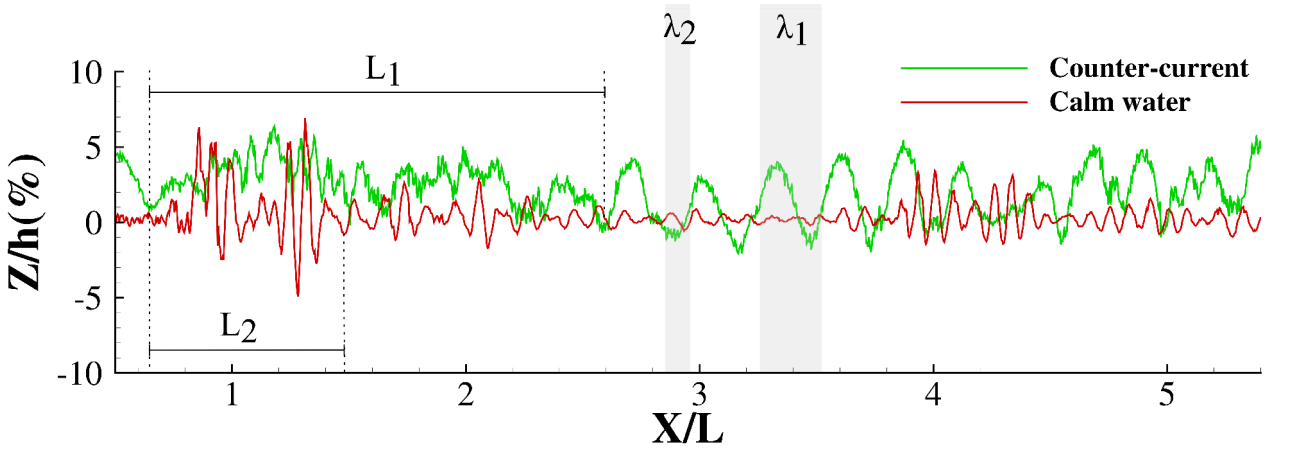

Figure 5: Longitudinal cut in the wake for a transverse position Y/B=3.5. Ship speed: U=0.45$m.s^{-1}$ – Counter-current speed : $|u|$=0.20$m.s^{-1}$.

4.2 Spectral analysis

One of the advantages of the stereo-refraction measurement method is that it gives a full reconstruction of the wake around the hull. Thus, the analysis of the measured wave fields can be extended in the spectral space [Gomit *et al.*, 2014 ; Caplier *et al.*, 2015b]. For that, a bidimensional discrete Fourier transform is conducted on the wake in the real space (O;X,Y), giving access to a representation of the wake in the spectral space (O;k_x,k_y). The resulting spectra are given on Figure 6, on which the left part corresponds to the calm water wake and the right to the counter-current configuration. The white line represents the theoretical solution of the dispersion relation calculated with equation (2). On the calm water wake spectrum, the energy is distributed between the branch corresponding to the dispersion relation calculated with a ship speed U=0.45$m.s^{-1}$, and the middle of the spectrum, corresponding to the near-field hydrodynamic mode around the hull [Gomit *et al.*, 2014 ; Caplier *et al.*, 2015b] (the cross in the middle of the spectrum is unphysical and is due to the calculation of the bidimensional discrete Fourier transform). As regards the counter-current case, the global energy in the spectrum is more important. The energy has shifted to the theoretical locus of the dispersion relation corresponding to a speed U+$|u|$=0.65$m.s^{-1}$ calculated with equation (4). So the theoretical

assumption on the change of reference frame in the dispersion relation is observed experimentally. In addition, there is a concentration of the energy around the cut-off wavenumber $k_x^c=g/U^2$, corresponding to the transverse wave number k_t. So this means that energy has been transferred to the transverse waves. In addition, the transverse wave number k_t has decreased, corresponding to an increase of the transverse waves wavelength. Both observations corroborate with the analysis in the real space. However, another branch , on which the energy is less important, has appeared in the spectrum (dotted line). That branch corresponds to the first harmonic of the dispersion relation and is not observed in the calm water spectrum. This non-linear effect should be caused by the saturation of the energy on the fundamental branch of the dispersion relation. The same phenomenon has been observed in previous experiments on deep and shallow water wakes in calm water (Figure 7), and compromises the definition of the wake angle in the real space [Caplier *et al.*, 2015b]. Indeed, both branches correspond to a different wake angle in the real space, and the resulting wake envelop does not form a V-shape. Thus, apart from the particular Kelvin wake pattern in deep water, the definition of a wake angle may not be relevant in other cases.

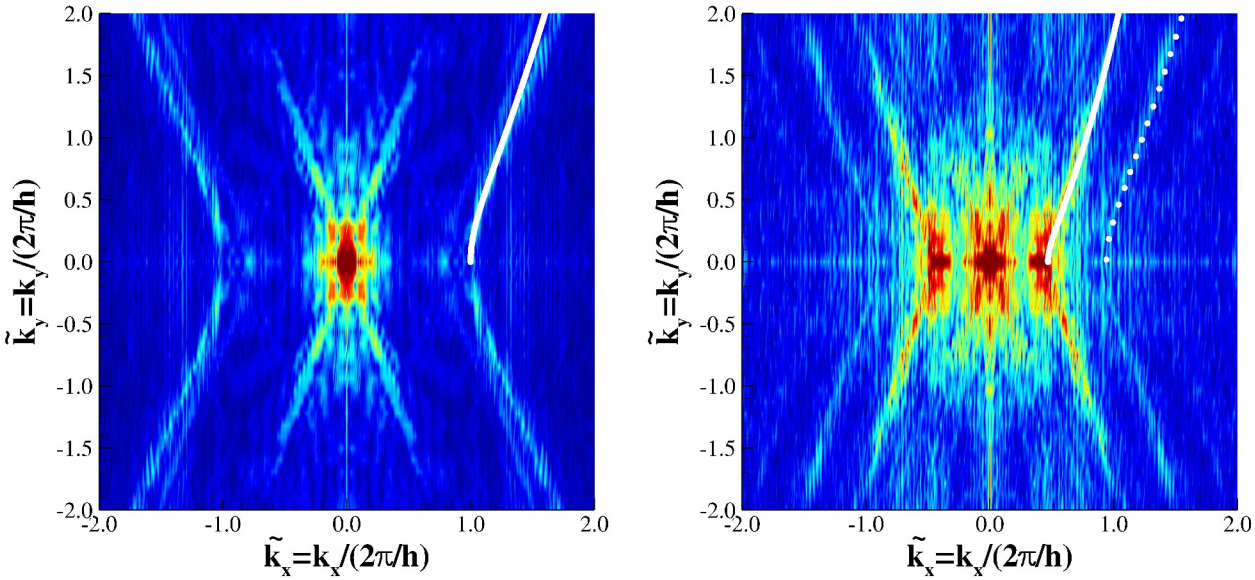

Figure 6: Spectral representation of the measured ship wakes. Left : calm water, right : counter-current. Ship speed: U=0.45$m.s^{-1}$ – Counter-current speed : $|u|$=0.20$m.s^{-1}$.

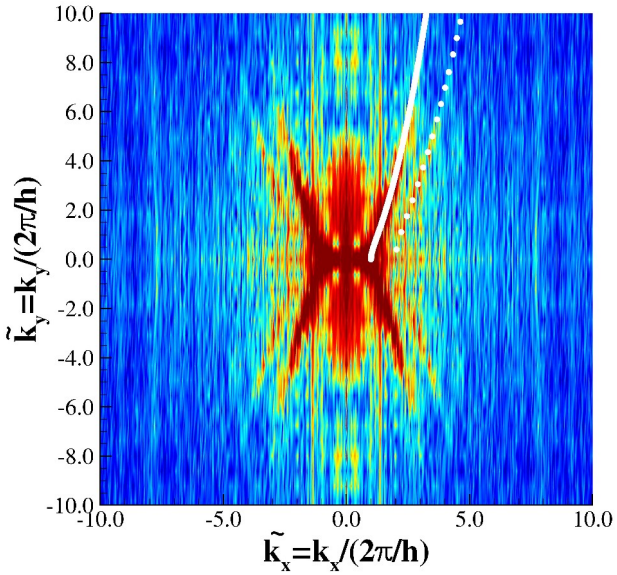

Figure 6: Spectral representation of the ship wake generated in deep water (h=0.483m) by the Wigley hull at a speed U=1.20$m.s^{-1}$ [Caplier *et al.*, 2015]. The first harmonic of the dispersion relation is visible in the spectrum.

5. CONCLUSIONS

The wakes generated by a parabolic ship hull in calm water and against a counter-current have been measured with a optical measurement method in a towing tank. The measured wave fields highlight the effects of the river counter-current on the ship wake. The widening of the wash zone on the river banks with the presence of a counter-current has been emphasized. In addition, the increasing of the wave resistance with the counter-current is observed through the increase of the wave amplitudes. As regards the transverse waves, the increase of their wavelength and also their amplitude has been identified and quantified in both real and spectral domain. The spectral analysis has highlighted the apparition of non-linear effects in the wake generated against a counter-current. This non-linear effects result in a widening of the wake envelop in the real space, compromising the notion of a wake angle. The analysis of the measured wakes in the real space also confirmed that the effect of the river counter-current, on an undulatory point of view, corresponds to a change of reference frame in the theoretical dispersion relation. The same study of ship wakes in the real and the spectral spaces should be now conducted in a co-current configuration, to investigate on the effect of the direction of the current. Finally, resistance tests in the presence of a current are necessary to conclude on its effects on ship resistance. Indeed, it is discussed in ancient literature, that the relation between the resistance in calm water $R=f(U)^2$ becomes $R=f(U\pm u)^2$ when the ship is navigating on a co- or counter-current [Tourasse and Mellet, 1828 ; Morin, 1855]. Although it has been shown that taking into account the current leads to simply changing the reference frame in the dispersion relation, governing the propagation of gravity waves, what about the ship resistance ?

REFERENCES

Bruschin J., Dysli M. (1974). – Erosion des rives due aux oscillations du plan d'eau d'une retenue – le Rhône à l'aval de Genève. *Bulletin technique de la Suisse romande*, **100(2)**:33-45.

Caplier C., Rousseaux G., Calluaud D., David L. (2015a). – An experimental study of the effects of finite water depth and lateral confinement on ships wake and drag. *Proceedings of the AIPCN-SHF congress "Hydrodynamics and simulation applied to inland waterway and port approaches".*

Caplier C., Rousseaux G., Calluaud D., David L. (2015b). – Energy distribution in ship wakes from a spectral analysis of the wave field : the deep and shallow water cases. *Submitted for publication*.

Carusotto I., Rousseaux G. (2013). – The Čerenkov effect revisited: from swimming ducks to zero modes in gravitational analogues. *Analogue Gravity Phenomenology, Springer International Publishing, Berlin*, **6**:109-144.

Crapper G.D. (1964). – Surface waves generated by a travelling pressure point. *Proc. R. Soc. Lond. A.*, **282(1391)**:547-558.

Ekman V.W. (1906). – On stationary waves in running water. *Ark. Mat. Astr. Fys.*, **3(2)**.

Ekman V.W. (1907). – On the waves produced by a given distribution of pressure which travels over the surface of water. *Ark. Mat. Astr. Fys.*, **3(11)**.

Ellingsen S.Å. (2014). – Ship waves in the presence of uniform vorticity. *J. Fluid Mech.*, **742**, R2.

Fang M.C., Yang R.Y., Shugan I.V. (2011). – Kelvin ship wake in the wind waves field and on the finite sea depth. *J. Fluid Mech.*, **27(01)**:71-77.

Gomit G., Rousseaux G., Chatellier L., Calluaud D., David L. (2014). – Spectral analysis of ship waves in deep water from accurate measurements of the free surface elevation by optical methods. *Phys. Fluids*, **26**:122101.

Gomit G., Chatellier L., Calluaud D., David L. (2013). – Free surface measurement by stereo-refraction. *Exp. Fluids*, **54**:1540.

Havelock T.H. (1908). – The propagation of groups of waves in dispersive media, with application to waves on water produced by a travelling disturbance. *Proc. R. Soc. Lond. A.*, **81(549)**:398-430.

Huygens C. (1937). – Oeuvres complètes de Christiaan Huygens. Mécanique théorique et physique de 1666 à 1965. *Dutch Society of Sciences*, **19(549)**:398-430.

Inui T. (Takao) (1955). – On the components of ship wave resistance. *Journal of Zosen Kiokai*, **1955(77)**:165-175.

Inui T. (Teturô) (1936). – On deformation, wave patterns and resonance phenomenon of water surface due to a moving disturbance. *Proc. Phys.-Math. Soc. Japan, III*, **18**:60-98.

Kelvin W.T. (Lord) (1887). – On ship waves. *Proc. Inst. Mech. Eng.*, **38(1)**:409.

Morin A. (1855). – Leçons de mécanique pratique : notions fondamentales de mécanique et données d'expériences. *Librairie Hachette et Cie, Paris*.

Tourasse, Mellet F.N., (1828). – Essai sur les bateaux à vapeur appliqués à la navigation intérieure et maritime de l'Europe. *Librairie Malher et Cie, Paris.*

Tremblais B., David L. (2010). – Standard Library for Image Processing software. http://sliplib.prd.fr/

Wigley W.C.S. (1926). – Ship wave resistance. A comparison of mathematical theory with experimental results. *Trans. of Royal Inst. of Nav. Arch.*, **14**:124-141.